ELSEVIER

Journal of Power Sources 92 (2001) 204–211

JOURNAL OF POWER SOURCES

www.elsevier.com/locate/jpowsour

Potassium manganese–vanadium oxide cathodes prepared by hydrothermal synthesis

Ping Liu*, Ji-Guang Zhang[1], John A. Turner

National Renewable Energy Laboratory, 1617 Cole Blvd., Golden, CO 80401, USA

Received 18 May 2000; accepted 11 June 2000

Abstract

Hydrothermal reactions between potassium permanganate and vanadyl sulfate have been used to synthesize new forms of vanadium oxides. Depending on the reactant ratios and pH values of the reaction mixtures, two different layered materials have been identified. The first one formed at a pH value of 1.6 has an interlayer distance of 10.90 Å and a composition of $K_{0.16}Mn_{0.04}V_2O_{4.94}{\cdot}0.14H_2O$, while the second one formed at pH values higher than 3.0 has an interlayer distance of 9.45 Å and a composition of $K_{0.44}V_2O_{4.96}$. Structural analysis indicates that they have a δ-type structure with potassium ions residing in between double sheets of vanadium oxide. The structure and composition of these materials have a profound effect on their charge and discharge properties when used as cathodes in lithium batteries. The sample prepared at a pH value of 2.3 shows best overall performance considering both reversible capacity and cyclability, which is explained with the coexistence of two layered phases in the material. This material has a capacity of over 200 mA h/g between 3.6 and 2.2 V and retains a capacity of 190 mA h/g after 30 cycles. Increase of manganese to vanadium ratio during synthesis leads to a gradual loss of the layered structure and decreased lithium insertion capacity.

Keywords: Potassium vanadium oxide; Manganese vanadium oxide; Hydrothermal synthesis; Lithium battery; Cathode materials

1. Introduction

Vanadium oxide and vanadium bronzes are among cathode materials with the highest reversible capacities for rechargeable lithium battery applications. Consequently, various forms of vanadium oxide have been studied extensively. These include crystalline and amorphous V_2O_5 [1–6], V_6O_{13} [7], V_6O_{14} [8], xerogels and aerogels [9–11], LiV_3O_8 [12,13] and vanadium bronzes such as sodium and potassium vanadium oxide [14,15]. Syntheses of these oxides involve either high-temperature solid-state processes or more preferably, low temperature approaches such as hydrothermal, sol–gel, and electrochemical methods [16,17].

Vanadium bronzes, including K, Na, Fe, Al, Cr, Cu, Zn, Mn, and Ni doped vanadium oxides have been synthesized and tested as cathodes in lithium batteries [14–25]. Several approaches have been adopted in the literature. The most common one utilizes the ion exchange properties of the vanadium oxide xerogel, which in turn is prepared by passing a sodium vanadate solution through a proton exchange resin. Subsequent high temperature treatment at 550°C leads to the formation of the β phase in the case of sodium and potassium [14,15]. Another approach involves the reaction between vanadium pentoxide and metal chloride. Bronzes formed after thermal treatment at 400°C have a general formula of M^{2+}-V_2O_5, where M = Ni, Mn, Co, and Cu [24].

In recent years, hydrothermal synthesis has received much attention for the preparation of metal oxides. Whittingham and co-workers successfully prepared layered lithium vanadium oxide and metal manganese oxides by using this technique [26–29]. The formation of vanadium oxide usually involves hydrothermal reduction of high valence vanadium compounds (vanadium oxide or sodium vanadate) in the presence of tetramethylammonium ions. Oka et al. employed the hydrothermal reactions between $VOSO_4$ and K_2SO_4 or $VO(OH)_2$ and KCl to prepare different potassium vanadium oxides [30–32]. Depending on the potassium/vanadium ratio, hydrated $K_{0.3}V_2O_5{\cdot}H_2O$ or unhydrated $K_{0{\cdot}5}V_2O_5$ could be obtained [30]. The combination of low temperature and high pressure in hydrothermal synthesis provides an opportunity to prepare metal oxides with

* Corresponding author. Tel.: +1-303-384-6503; fax: +1-303-384-6655.
E-mail address: ping_liu@nrel.gov (P. Liu).
[1] Present address: Macro Energy-Tech Inc., Redondo Beach, CA 90278, USA.

0378-7753/01/$ – see front matter
PII: S0378-7753(00)00542-5

new structures. In this report, we show that new forms of layered vanadium oxide can be synthesized through a simple hydrothermal reaction between potassium permanganate and vanadyl sulfate. These compounds show a high discharge capacity and excellent stability when tested as cathodes in lithium batteries. Characterization of the materials by XRD, TGA, SEM and FTIR are also presented.

2. Experimental

Vanadium oxide has been synthesized by using the reaction between potassium permanganate and vanadyl sulfate. In a typical synthesis, a solution of 0.158 g of $KMnO_4$ in 20 g of water is slowly added to a solution of 2.14 g of $VOSO_4{\cdot}3H_2O$ in 10 g of water. If necessary, the pH value of the mixture is adjusted by adding sulfuric acid or a potassium hydroxide solution. After stirring for 20 min, the mixture is then transferred to a Teflon-lined autoclave and heated at 170°C for 4 days. The autoclave is then quenched in water and the mixture is filtrated and washed with large amount of water; and the remaining compound is dried at 80°C.

The compositions of the materials were determined by inductively coupled plasma emission spectroscopy (ICP). The oxidation states of vanadium and manganese were obtained by redox titration with 0.02 M $KMnO_4$ after the sample powder was dissolved in 14.3 vol.% dilute sulfuric acid. For samples with manganese oxidation state higher than +2, known amount of $VOSO_4{\cdot}3H_2O$ was added to dissolve the sample and $KMnO_4$ was then used to titrate the remaining VO^{2+}. X-ray diffraction (XRD) measurements were performed at 2°C/min on a 4-circle Scintag X-1 Diffractometer with a Cu Kα anode source. Thermogravimetric analyses (TGA) were performed in oxygen on a TGA 51 analyzer at a ramping rate of 10°C/min. Infrared (IR) spectra were collected on a Midac PRS 933 infrared spectrophotometer. Scanning electron micrographs (SEM) were obtained on a JSM scanning electron microscope.

To fabricate an electrode for electrochemical testing, the vanadium oxide powder was mixed with acetylene black and a solution of poly(vinyliedene fluoride) (PVDF) in 1-methyl-2-pyrrolidinone. After forming slurry, the mixture was spread on a nickel mesh using a spatula. The electrode was then dried under vacuum at 120°C for 12 h. The final electrode consisted of 60% active material, 30% carbon black, and 10% PVDF by weight. The area of the electrode was 1 cm^2 and the weight of active material in an electrode was typically ∼10 mg. A three-electrode cell was used to test its electrochemical properties, and lithium metal was used as both the counter and reference electrodes. A solution of 1 M $LiClO_4$ in propylene carbonate was used as the electrolyte during the electrochemical measurement. Cycling tests were performed at a 29.4 mA/g rate on a BT-2043 Arbin battery testing system (Arbin Instruments, TX).

3. Results and discussion

3.1. Syntheses and characterization of K-Mn-V-O compounds

The first set of samples was prepared using the above-mentioned typical procedure, where Mn to V ratio was 0.1. The pH values of the final mixture were adjusted to 1.6, 2.3, 3.0, and 4.0, respectively. Fig. 1 shows the XRD patterns of the four samples. The broad background (10–30°) is an artifact due to the use of scotch tape/glass substrate during the measurement. The material formed at a pH value of 1.6 exhibited a layered structure similar to the δ-$K_{0.3}V_2O_5{\cdot}H_2O$ obtained by Oka et al. (10.88 Å) [30]. The d structure featured double sheets of vanadium oxide in between which potassium ions reside. When the pH value was increased to 2.3, a second layered phase evolved with an interlayer distance of 9.45 Å. This value was very similar to that of δ-$K_{0.5}V_2O_5$ synthesized by Oka et al. (9.50 Å) [30]. If the pH value was further increased to 3.0 and 4.0, the first layered phase completely disappeared. ICP analyses revealed that for the samples prepared at pH values higher than 2.3, there was no manganese in the materials, and the K to V ratios were ∼0.22. The material prepared at a pH of 1.6 had a K:Mn:V ratio of 0.08:0.02:1. The fact that no phase from manganese oxide could be found suggested that a layered K-Mn-V-O compound was formed.

TGA measurements were performed on these samples in oxygen (Fig. 2). Appreciable weight loss was only observed for the first sample (pH = 1.6). The result from the other samples was similar (the plot for the sample prepared at a pH value of 3.0 was not shown for clarity). The first sample lost 1.1% of the initial weight up to 100°C, which could be attributed to the release of loosely bonded water. More tightly bonded water was lost over a wide temperature range from 100 to 400°C. A total of 2.8% of weight was lost up to

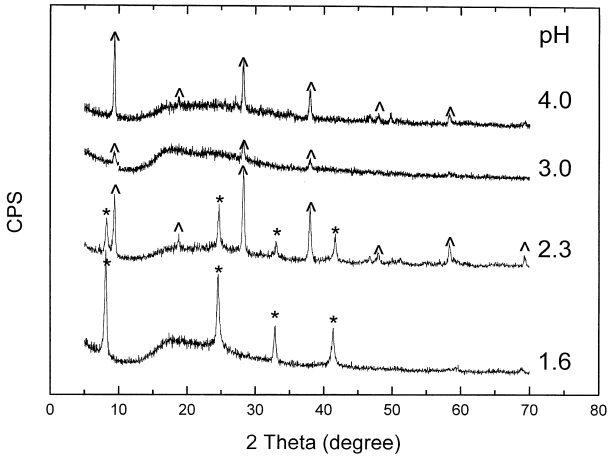

Fig. 1. XRD patterns of four samples prepared at different pH values of the mixture. ∗ and ^ signs denote the 0 0 *l* diffraction peaks of two layered phases.

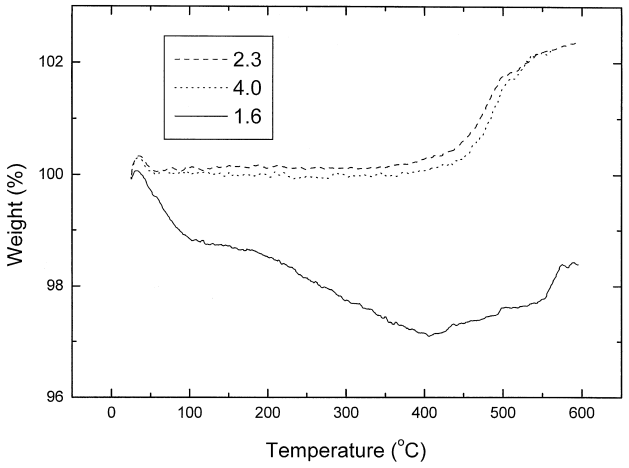

Fig. 2. TGA plots of three samples prepared at different pH values.

400°C. Above that temperature, a weight gain of 1.3% was observed.

Redox titration was used to determine the oxidation states of vanadium and manganese. The composition of the compound could then be estimated to be $K_{0.16}Mn_{0.04}V_2O_{4.94}{\cdot}0.14H_2O$. For the samples prepared at pH values of 2.3–4.0, the compositions could be estimated as $K_{0.44}V_2O_{4.96}$. These compositions correlated very well with the weight gain observed in TGA experiments where the highest oxidation state of vanadium (+5) was obtained after heat treatment in oxygen at high temperature. In addition, the composition of $K_{0.44}V_2O_{4.96}$ distinguishes the sample from potassium exchanged vanadium oxide xerogels and the bronzes prepared from it by high temperature treatment. The maximum exchange capacity of the xerogel is limited to 0.36 mole K^+ per V_2O_5 unit and the resultant bronze usually has a composition of $K_{0.25}V_2O_5$ [15]. On the other hand, it is very close to the unhydrated compound δ-$K_{0.5}V_2O_5$ reported by Oka et al. [30].

Infrared (IR) spectra of the four samples are shown in Fig. 3. Vanadium oxide has an absorption band at 1022 cm^{-1} that is attributed to the vibration of the V=O bond. A shift of this band would indicate changes of the oxidation state of vanadium and the coordination around it [33]. The material prepared at a pH of 1.6 featured absorption bands at 1018 and 721 cm^{-1}, which were similar to those of δ-V_2O_5, with the 1018 cm^{-1} absorption indicative of a distorted octahedron configuration [34]. As the pH value was raised to 2.0 and 3.0, a series of absorption bands at 1001, 968, 950, and 941 cm^{-1} were developed at the expense of the 1018 cm^{-1} band. This observation was consistent with the decrease in oxidation state of vanadium, which led to a red shift of IR bands. All of the four bands could be attributed to different V=O vibrations, indicating that there were four types of vanadium coordination in this compound. In summary, XRD, IR and compositional analysis indicated that potassium vanadium oxides prepared by our method might have a δ-type structure, in which potassium ions reside in between double sheets of vanadium oxide [30–32,34].

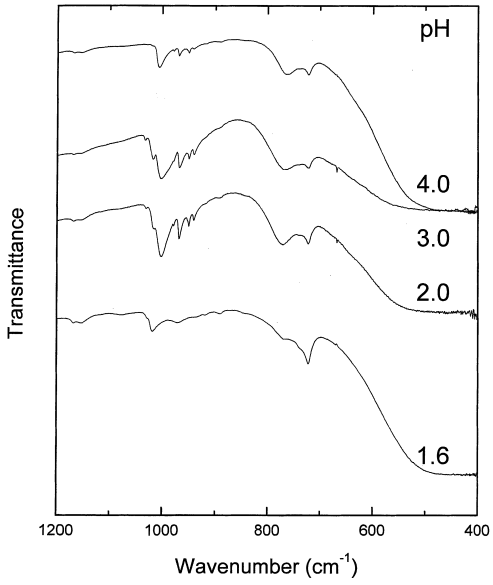

Fig. 3. IR spectra of the four samples prepared at different pH values.

The second set of samples was prepared with potassium permanganate to vanadyl sulfate ratios (Mn/V ratios) varied from 0.1 to 1 in the starting mixture without any adjustment of pH values (pH $\approx$ 1.6). Fig. 4 shows the XRD patterns of the four samples. Increase of the Mn/V ratio from 0.1 to 0.15 in the reactants led to a similar material. As the Mn/V ratio was further increased to 0.2, only a series of broad diffraction peaks were observed. The pattern was very similar to that of vanadium oxide xerogel prepared in an alcoholic solution [35]. When the Mn/V ratio was raised to 1:1, the layered structure was no longer visible and the material was essentially amorphous.

ICP analyses revealed that K:Mn:V ratios in the resultant compounds were 0.08:0.02:1, 0.11:0.02:1, 0.01:0.09:1, and 0.26:1.11:1, respectively. The very low content of manganese in the first two samples indicated that most of the

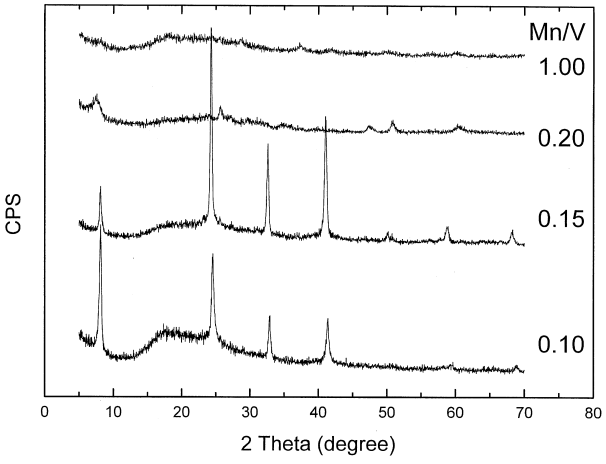

Fig. 4. XRD patterns of four samples prepared with different molar ratios of Mn to V in the starting mixture. The pH values are 1.6.

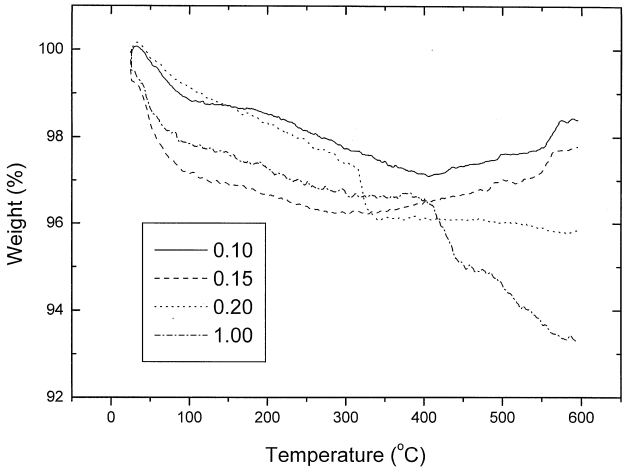

Fig. 5. TGA plots of the four samples prepared with different molar ratios of Mn to V in the starting mixture.

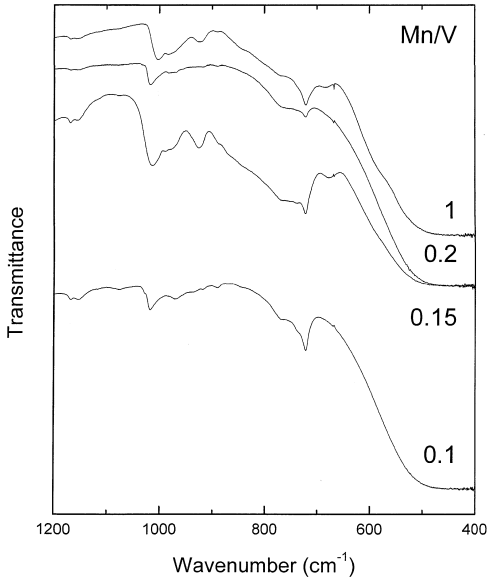

Fig. 6. IR spectra of the four samples prepared with different molar ratios of Mn to V in the starting mixture.

manganese was reduced to a soluble Mn^{2+} state. Manganese content increased with increasing amount of permanganate as expected and reached a Mn/V ratio of 1.11 in the last sample. This was due to the excess amount of permanganate, which did not favor the formation of a soluble Mn^{2+} species. TGA spectra of these samples are shown in Fig. 5. The first two samples (Mn/V = 0.1 or 0.15) exhibited similar patterns, however, the water content in the second sample was 0.33 mol per V_2O_5 as compared to 0.14 mol in the first sample. Dramatic changes were observed for the sample prepared with a Mn/V ratio of 0.2. 2.7% of the weight was lost before 313°C, where a rapid weight loss of 1.3% occurred. This pattern was very similar to that of vanadium oxide xerogels, except that the water loss was substantially lower for this material (xerogel could lose up to 20%) [34]. The rapid loss at 320°C was attributed to the crystallization of orthorhombic V_2O_5, when strongly bonded water was released. The sample prepared at a Mn/V ratio of 1 lost 7% of the weight to 600°C and a rapid mass loss was observed at around 425°C. Considering the results from oxidation state measurements and TGA results we estimated their formulae as $K_{0.16}Mn_{0.04}V_2O_{4.94}{\cdot}0.14H_2O$, $K_{0.22}Mn_{0.04}V_2O_{5.02}{\cdot}0.33H_2O$, $K_{0.02}Mn_{0.18}V_2O_{5.19}{\cdot}0.48H_2O$, and $K_{0.52}Mn_{2.22}V_2O_{9.30}{\cdot}1.15H_2O$, respectively. It is worth noting that manganese with oxidation state higher than +2 could not coexist with V(IV) species. As the amount of permanganate increases, the oxidation state of vanadium increased from 4.82 to 4.87 to 5.00 while manganese remained as Mn(II), after which the oxidation state of manganese increased from 2 to 3.64 with vanadium as V(V).

Fig. 6 shows the IR spectra of the four samples. As the permanganate amount was increased, the band for the V=O vibration (1000 cm^{-1}) shifted to higher wavenumber, which was consistent with an increase in the oxidation state of vanadium. The similarity of the patterns of the spectra also indicated that vanadium coordination in the four samples were quite similar.

Two representative samples were also examined by scanning electron microscopy (Fig. 7). The samples were first dispersed in acetone by ultrasonication and then coated on copper grid for measurement. The first sample (pH = 1.6) shows uniform long plates of over 8 μm long and 0.5 μm wide. These shapes are consistent with its layered structure as observed in the XRD patterns. The second sample (pH = 4) also shows plate-like morphology but with smaller size and irregular shape.

3.2. Electrochemical properties

The first-cycle charge and discharge curves of the four samples prepared at different pH values are shown in Fig. 8a–d. The insets show the differential curves, which can illustrate the phase transitions during cycling. The well-defined plateaus in the discharge curves indicate that these materials are different from vanadium oxide xerogels, which always show featureless discharge profiles [16]. The sample prepared at a pH of 1.6 (Fig. 8a) exhibits three distinct discharge processes at 3.2, 2.75 and 2.55 V versus Li, respectively. The first process at 3.2 V is not reversible as indicated by the absence of a de-intercalation peak during charging.

The sample prepared at a pH value of 2.3 (see Fig. 8b) shows different behavior. The ill-defined discharging process above 3 V is developed into a well-defined de-intercalation process in the charging step as shown by the peak at 3.25 V. The intercalation process at 2.55 V splits into two plateaus at 2.6 and 2.65 V upon charging, which also appear for the subsequent two samples. The charge delivered at the low potential plateau (2.5 V) is only partially reversible, which contributes to the low Coulomb efficiency. The

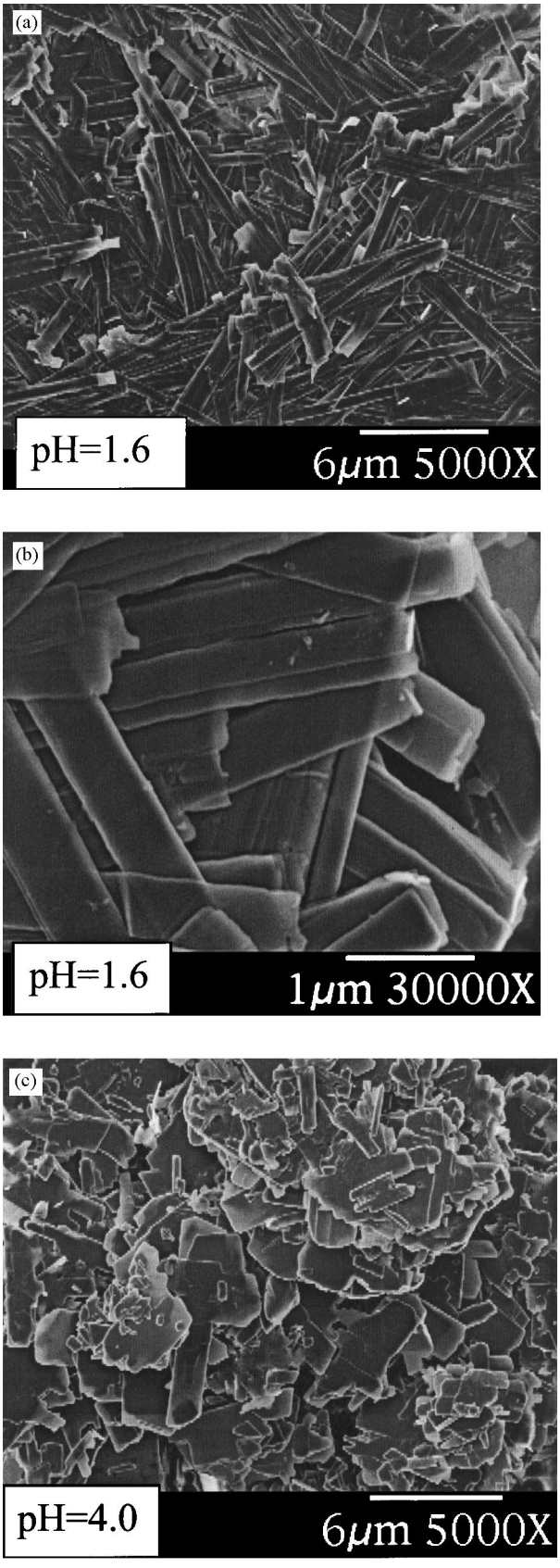

Fig. 7. Scanning electron micrographs of two samples prepared at pH values of 1.6 and 4.0 as in Fig. 1.

differences in the samples can be better illustrated by comparing the first sample (pH = 1.6) with the others (pH = 2.3, 3, and 4). There is no splitting process in the first sample and the process at 2.55 V is highly reversible. The broadness of the $-\mathrm{d}C/\mathrm{d}V$ versus V curve for the first sample also indicates that there is an energetic distribution of the intercalation sites, which is in strong contrast with those shown in the other samples.

Based on the structural information obtained from XRD and composition analysis, we concluded that the compound $K_{0.44}V_2O_{4.96}$ may have a structure similar to δ-$K_{0.5}V_2O_5$ reported before [30]. However, no electrochemical data are available from the literature for a direct comparison. Whittingham et al. reported on the lithium insertion properties of $Zn_{0.4}V_2O_5{\cdot}0.3H_2O$ that also has a δ type of structure [34]. While the initial lithium insertion capacity is similar (about 0.6–0.7 Li/V), the discharge profiles are different, indicating the difference in lithium insertion sites.

The cycling behavior of the four samples is shown in Fig. 9. The sample prepared at a pH of 1.6 demonstrates good capacity retention with a reversible capacity value of 190 mA h/g. The sample prepared at a pH of 3.0 shows very high initial capacity of over 300 mA h/g, however, with a subsequent fast degradation. Further increase of the pH to 4.0 results in a large capacity decrease while the subsequent degradation is still serious. The best sample is the one prepared at a pH value of 2.3; a large capacity of over 200 mA h/g between 2.2 and 3.6 V and good cycling stability are obtained simultaneously. This might be due to the coexistence of two layered structures as indicated by the XRD results. The first layered structure is very reversible for lithium intercalation as shown by the first sample (pH = 1.6), while the second layered structure has a higher lithium storage capacity as shown in the third sample (pH = 3.0). A combination of the two structures provides the optimal results. The charge capacity of this material is comparable to that of potassium vanadium bronze [15] under similar discharging conditions.

The charge and discharge behavior of the materials prepared at different Mn to V ratios was also investigated (Fig. 10a and b). The samples prepared at Mn/V ratios of 0.1 and 0.15 show similar profiles (not shown). A dramatic change is observed when the Mn to V ratio is increased to 0.2 (Fig. 10a). Only two processes at 2.5 and 2.8 V can be seen, both of them being only partially reversible. As a result, the overall reversible capacity is very low (less than 100 mA h/g). Upon further increase of the Mn to V ratio to 1:1, the intercalation potentials are slightly higher and the two processes are more reversible. It is believed that in the third sample (Fig. 10a), the layered structure may begin to collapse due to the excessive oxidation of vanadium species and some of the intercalation sites are eliminated, which contributes to the low capacity. Further structural analyses, however, are in need to elucidate the lithium insertion process.

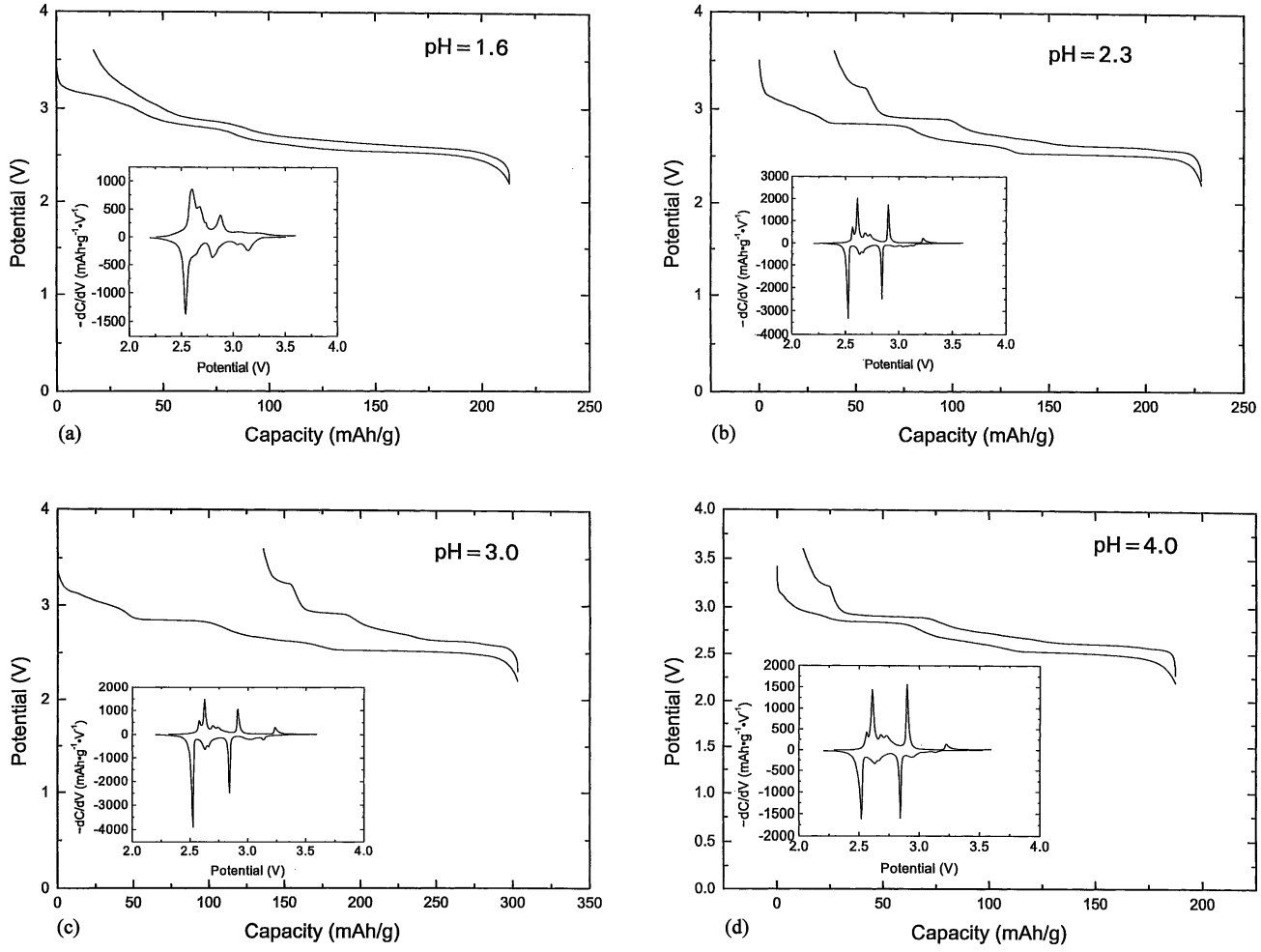

Fig. 8. The first-cycle charge and discharge curves of the four samples prepared at different pH values. The insets show the $-\mathrm{d}C/\mathrm{d}V$ differential curves and a–d designations correspond to pH values of 1.6, 2.3, 3.0, and 4.0, respectively.

Cycling data of the samples are presented in Fig. 11. Higher capacities are obtained for the first two samples, while the sample prepared with a Mn to V ratio of 0.1 exhibits the best capacity retention. Although its capacity is quite low, the sample prepared with a Mn to V ratio of 0.2 shows excellent cycling stability.

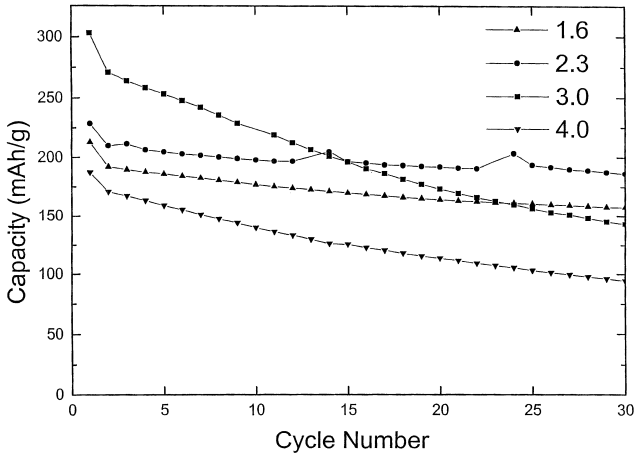

Fig. 9. Cycling behavior of the samples prepared at different pH values.

4. Conclusions

A simple redox reaction between potassium permanganate and vanadyl sulfate has been used to prepare novel vanadium oxides. Depending on the pH values of the solution and the Mn to V ratio in the reaction mixture, two types of layered phases or a mixture of them have been observed. Compositional analyses and XRD results indicate that the $K_{0.44}V_2O_5$ obtained in this work may have a δ-type structure where potassium ions reside in between double sheets of vanadium oxide. Cycling in lithium batteries show that the material composed of the mixture of the two layered phases exhibits high charge and discharge capacities of over 200 mA h/g between 3.6 and 2.2 V and excellent cycling stability with a capacity of 190 mA h/g after 30 cycles. Increasing the Mn/V ratio in the synthesis leads to the loss of the layered structure and decreased lithium insertion

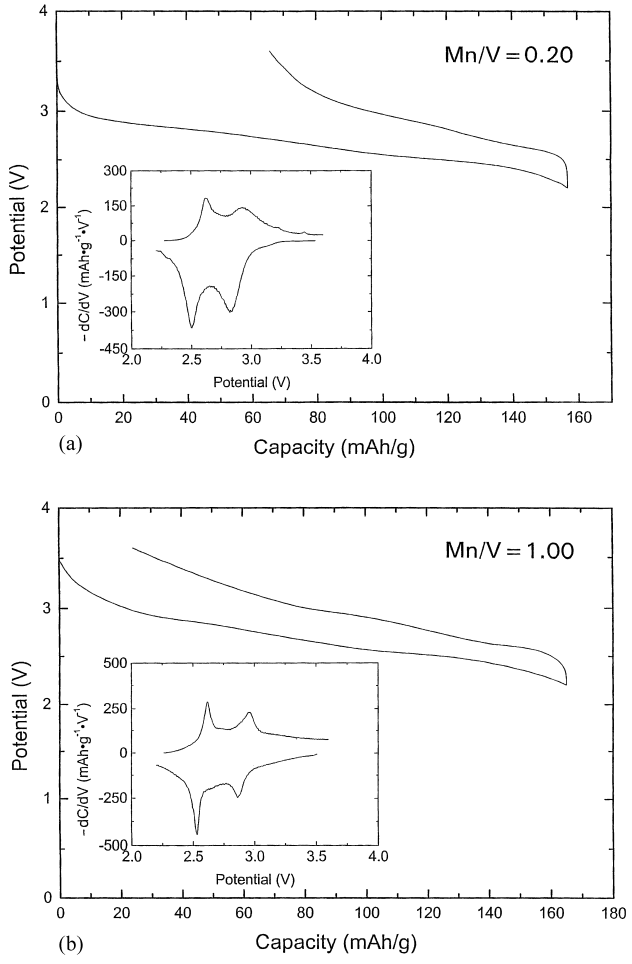

Fig. 10. The first-cycle charge and discharge curves of the four samples prepared with different Mn/V ratios. The insets show the $-dC/dV$ differential curves and a–b designations correspond to Mn/V ratios of 0.2 and 1, respectively.

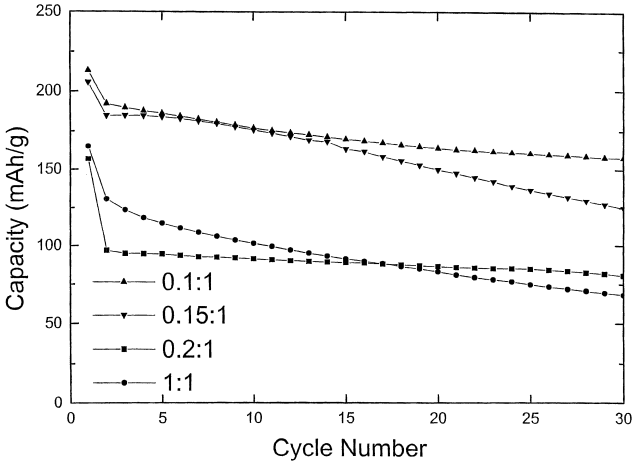

Fig. 11. Cycling behavior of the four samples prepared at different Mn/V ratios.

capacity. These layered materials may find applications as cathodes for rechargeable lithium batteries.

Acknowledgements

This work has been supported by the Advanced Battery Program, Office of Basic Energy Sciences, US Department of Energy under contract No. DE-AC-36-83CH10093. We thank Mr. C. Edwin Tracy for his comment on the manuscript.

References

[1] D.W. Murphy, P.A. Christian, F.J. Disalvo, J.V. Waszczak, Inorg. Chem. 18 (1979) 2800.
[2] P.G. Dickens, S.J. French, A.T. Hight, M.F. Pae, Mater. Res. Bull. 14 (1979) 1295.
[3] Y. Sakurai, J.-I. Yamaki, J. Electrochem. Soc. 135 (1988) 791.
[4] M.S. Whittingham, J. Electrochem. Soc. 123 (1976) 315.
[5] C. Delmas, H. Cognac-auradou, J.M. Cocciantelli, M. Menetrier, J.P. Dourmerc, Solid State Ionics 69 (1994) 257.
[6] K. Wiesener, W. Schncider, D. Ilic, E. Steger, K.H. Hallmeir, E. Brackmann, J. Power Sources 20 (1978) 157.
[7] D.W. Murphy, J.N. Carides, F.J. Disalvo, J.V. Waszcak, Mater. Res. Bull. 13 (1978) 1395.
[8] M.Y. Saidi, R. Koksbang, E.S. Saidi, J. Barker, Electrochem. Acta 42 (1997) 1181.
[9] R. Baddour, J.P. Pereira-Ramos, R. Messina, J. Perichon, J. Electroanal. Chem. 314 (1991) 81.
[10] H.K. Park, W.H. Smyrl, M.D. Ward, J. Electrochem. Soc. 142 (1995) 1068.
[11] D.B. Le, S. Passerini, F. Coustier, J. Guo, T. Soderstrom, B.B. Owens, W.H. Smyrl, Chem. Mater. 10 (1998) 682.
[12] M. Pasquali, G. Pistoia, V. Manev, R.V. Moshtev, J. Electrochem. Soc. 133 (1986) 2454.
[13] N. Kumagai, A. Yu, J. Electrochem. Soc. 144 (1997) 830.
[14] J.P. Pereira-Ramos, L. Znaidi, N. Baffier, R. Messina, Solid State Ionics 28–30 (1988) 886.
[15] S. Maingot, N. Baffier, J.P. Pereira-Ramos, P. Willmann, Solid State Ionics 67 (1993) 29.
[16] J.P. Pereira-Ramos, N. Baffier, G. Pistoia, in: G. Pistoia (Ed.), Lithium Batteries, New Materials, Developments and Perspectives, Elsevier, The Netherlands, 1994, p. 287.
[17] Y. Sato, T. Nomura, H. Tanaka, K. Kobayakawa, J. Electrochem. Soc. 138 (1991) L37.
[18] T. Watanabe, A. Shimizu, M. Inagaki, J. Mater. Chem. 5 (1995) 753.
[19] J.J. Legendre, P. Aldebert, N. Baffier, J. Livage, J. Colloid Interface Sci. 94 (1983) 84.
[20] M. Inagaki, K. Omori, T. Tsumura, T. Watanabe, A. Shimizu, Solid State Ionics 78 (1995) 275.
[21] S. Maingot, R. Baddour, J.P. Pereira-Ramos, N. Baffier, P. Willmann, J. Electrochem. Soc. 140 (1993) L158.
[22] R. Baddour-Hadjean, J. Farcy, J.P. Pereira-Ramos, N. Baffier, J. Electrochem. Soc. 143 (1996) 2083.
[23] P. Soudan, J.P. Pereira-Ramos, G. Gregoire, N. Baffier, Ionics 3 (1997) 261.
[24] M. Inagaki, K. Omori, T. Tsumura, A. Shimizu, Solid State Ionics 86 (1996) 849.
[25] M.Y. Saidi, J. Barker, E.S. Saidi, R. Koksbang, Solid State Ionics 82 (1995) 203.
[26] T. Chirayil, P. Zavalij, M.S. Whittingham, Solid State Ionics 84 (1996) 163.

[27] T. Chirayil, P. Zavalij, M.S. Whittingham, Chem. Mater. 10 (1998) 2629, and references therein.
[28] R.J. Chen, M.S. Whittingham, J. Electrochem. Soc. 144 (1997) L64.
[29] F. Zhang, P. Zavalij, M.S. Whittingham, Electrochem. Commun. 1 (1999) 564.
[30] Y. Oka, T. Yao, N. Yamamoto, J. Mater. Chem. 5 (1995) 1423.
[31] T. Yao, Y. Oka, N. Yamamoto, J. Mater. Chem. 2 (1992) 331.
[32] Y. Oka, T. Yao, N. Yamamoto, J. Mater. Chem. 3 (1993) 1037.
[33] G.G. Janauer, A. Dobley, J. Guo, P. Zavalij, M.S. Whittingham, Chem. Mater. 8 (1996) 2096.
[34] F. Zhang, P.Y. Zacalij, M.S. Whittingham, Mater. Res. Bull. 32 (1997) 701.
[35] A. Davues, R.J. Hobson, M.J. Hudson, W.J. Macklin, R.J. Neat, J. Mater. Chem. 6 (1996) 49.